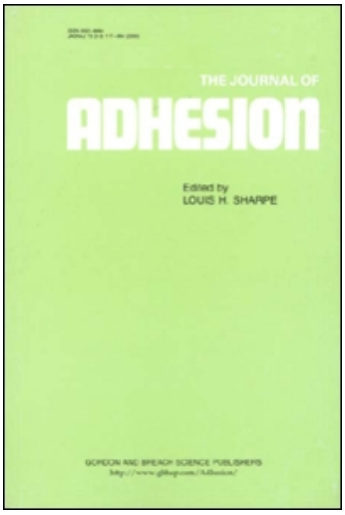

The Journal of Adhesion
Publication details, including instructions for authors and subscription information:
http://www.informaworld.com/smpp/title~content=t713453635

Chemistry-Specific Interfacial Forces Between Barnacle (*Semibalanus Balanoides*) Cyprid Footprint Proteins and Chemically Functionalised AFM Tips

In Yee Phang[abc]; Nick Aldred[d]; Xing Yi Ling[e]; Nikodem Tomczak[ac]; Jurriaan Huskens[e]; Anthony S. Clare[d]; G. Julius Vancso[ab]
[a] Department of Materials Science and Technology of Polymers and MESA+ Institute for Nanotechnology, University of Twente, Enschede, The Netherlands [b] Dutch Polymer Institute, Eindhoven, The Netherlands [c] Institute of Materials Research and Engineering, 3 Research Link, Singapore 117602 [d] School of Marine Science and Technology, Newcastle University, Newcastle upon Tyne, UK [e] Molecular Nanofabrication Group and MESA+ Institute for Nanotechnology, University of Twente, Enschede, The Netherlands

To cite this Article Phang, In Yee , Aldred, Nick , Ling, Xing Yi , Tomczak, Nikodem , Huskens, Jurriaan , Clare, Anthony S. and Vancso, G. Julius(2009) 'Chemistry-Specific Interfacial Forces Between Barnacle (*Semibalanus Balanoides*) Cyprid Footprint Proteins and Chemically Functionalised AFM Tips', The Journal of Adhesion, 85: 9, 616 — 630
To link to this Article: DOI: 10.1080/00218460902996952
URL: http://dx.doi.org/10.1080/00218460902996952

The Journal of Adhesion, 85:616–630, 2009

ISSN: 0021-8464 print/1545-5823 online
DOI: 10.1080/00218460902996952

Taylor & Francis
Taylor & Francis Group

Chemistry-Specific Interfacial Forces Between Barnacle (*Semibalanus Balanoides*) Cyprid Footprint Proteins and Chemically Functionalised AFM Tips

In Yee Phang[1,2], Nick Aldred[3], Xing Yi Ling[4], Nikodem Tomczak[1], Jurriaan Huskens[4], Anthony S. Clare[3], and G. Julius Vancso[1,2]

[1]Department of Materials Science and Technology of Polymers and MESA$^+$ Institute for Nanotechnology, University of Twente, Enschede, The Netherlands
[2]Dutch Polymer Institute, Eindhoven, The Netherlands
[3]School of Marine Science and Technology, Newcastle University, Newcastle upon Tyne, UK
[4]Molecular Nanofabrication Group and MESA$^+$ Institute for Nanotechnology, University of Twente, Enschede, The Netherlands

Cypris larvae of the barnacle Semibalanus balanoides *leave proteinaceous footprints on surfaces during pre-settlement exploration. These footprints are considered to mediate temporary adhesion of cyprids to substrata and, as such, represent a crucial first step in the colonization of man-made surfaces by barnacles, a process known as biofouling. Interest in this system also stems from the potential for a synthetic reversible adhesion system, based on the strategy used by cyprids. Cyprid footprints were probed using atomic force microscopy (AFM) and nanomechanical data relating to interfacial adhesion forces were correlated with AFM tip chemistry. Commercial Si_3N_4-tips and chemically functionalized CH_3-tips were chosen to mimic the interactions of cyprid footprints with hydrophilic and hydrophobic surfaces, respectively. Force-extension curves of protein bundles picked up by AFM tips exhibited a characteristic saw-tooth appearance for both types of tip, but demonstrated clear differences relating to pull-off force and pull-off length, based on tip chemistry. Additional (~6 nN) interfacial adhesion forces between $-CH_3$ functionalized tips and footprints were assigned to hydrophobic interactions.*

Received 3 October 2008; in final form 2 April 2009.

One of a Collection of papers honoring J. Herbert Waite, the recipient in February 2009 of *The Adhesion society Award for Excellence in Adhesion Science, Sponsored by 3M*.

Present address of Nikodem Tomczak and In Yee Phang is Institute of Materials Research and Engineering, 3 Research Link, Singapore 117602.

Address correspondence to Nick Aldred, School of Marine Science and Technology, Newcastle University, Newcastle upon Tyne, NE1 7RU, UK. E-mail: nicholas.aldred@ncl.ac.uk

Footprint proteins adhered with greater tenacity to the hydrophobic tip. This may suggest conformational change and denaturing of the protein which would facilitate hydrophobic interaction by enhancing contact forces between $-CH_3$ functionalized tips and hydrophobic groups in the footprint molecule(s). Neither tip removed proteins from the $-NH_2$ substratum suggesting that specific chemical interactions, rather than simple wetting phenomena, govern the adhesion of footprint proteins to that surface.

Keywords: Antifouling; Atomic force microscopy (AFM); Barnacle; Cyprid; Fouling; *Semibalanus balanoides*; Temporary adhesion

INTRODUCTION

For decades, the incentive to research barnacles and their adhesion has stemmed from their role as important biofouling organisms [1]. The accumulation of fouling on the hulls of ships has the principal effect of increasing surface roughness and, therefore, increasing hydrodynamic drag [2]. Depending on the affected structure, other effects enhanced are corrosion [3], increased greenhouse gas emissions [4], reduced propulsion efficiency, and increased fuel costs (by up to 86%) [2]. There is an alternate perspective, however, that has been less well explored in the literature. Barnacles are also of interest to those who wish to exploit their adhesives commercially [5]. In this regard, the cypris larva of barnacles, which has adhesives that are discrete from those of the adult, has received surprisingly little attention.

The cyprid is the seventh and final larval stage in the life cycle of thoracican barnacles and is responsible for surface exploration, surface selection, and settlement [6,7]. Cyprids are capable of rapidly reversible adhesion to immersed surfaces, a process referred to usually as "temporary adhesion". Temporary adhesion is used during the initial exploration of surfaces by a cyprid in order to identify surfaces that meet the requirements for settlement [8]. Using two specialized antennules, bearing sensory structures [9] and terminated in an adhesive disc [10], cyprids walk across surfaces in a bi-pedal fashion and at a maximum rate of two body lengths per second [7]. During surface exploration, "footprints" of a glycoproteinaceous material are deposited and this material has an assumed role in the temporary adhesion of the organism, in some cases being termed "temporary adhesive" [8] although its role as such has never been firmly established [8]. Once the cyprid commits to settlement, a rapidly curing permanent cement [11] is secreted through the antennules, embedding them and fixing the cyprid permanently to the surface. The permanent cement, which is not discussed any further in this study, is thought to differ in

composition and function to both the footprint material and the adult barnacle cement [7,12]. Metamorphosis from a settled cyprid to a juvenile barnacle is then completed within a matter of hours.

Understanding the temporary adhesion of barnacle cyprids would be a useful step towards the development of biomimetic adhesives that are capable of functioning underwater—an area of adhesion science that has, historically, proven to be a problem area [13]. Footprints deposited onto surfaces by cyprids have two interfaces, namely, the protein–substratum interface and the protein–seawater interface; the latter of which is in contact with the cyprid antennular disc during adhesion [7]. This system, therefore, provides a rare model for studying the properties and composition of a reversible adhesion system that has evolved to function in a liquid medium. The present study concentrates on the footprint material of cyprids and builds on information presented in recent publications [14–16]. We explore, using atomic force microscopy (AFM)-based molecular force spectroscopy, the adherence of the footprint material to AFM tips bearing two different wettabilities, either hydrophilic or hydrophobic.

AFM is conceptually an uncomplicated but versatile technique [17]. In its most simple application, AFM employs a sharp probe to image surface topology on the micro-/nano-scale. Most commonly, the surface of interest is raster scanned in relation to a static tip—a process controlled by electronic feedback. Reflection of a laser beam from the AFM tip is detected and this information can be interpreted into x, y, and z data allowing real-time compilation of high-resolution three-dimensional topological maps. Force-distance interactions between the tip and the surface can also be measured to high sensitivity, providing that the spring constant of the cantilever (onto which the tip is mounted) is known. The advantages of AFM over other microscopic techniques have been exploited previously to measure surface topology of samples in three dimensions [18,19], surface physical/chemical properties [20,21], and physical properties of (bio)macromolecules at the nano-scale and in different environments [22–39]. For homogeneous protein films, single protein chains can be stretched and force-extension curves can be measured quantitatively (for a recent review see, *e.g.,* Ref. [40]), although for native biological samples it is almost inevitable that numerous protein chains will be pulled simultaneously. There is, however, growing interest in using AFM-based techniques to measure the mechanical properties of macromolecules *in singulo*, so as to study the static and dynamic molecular properties of engineered proteins, measure specific antigen-antibody interactions, and determine the energy dissipation associated with bond rupturing [24–30]. In addition,

the surface of the AFM tip can be tailored by chemical functionalization for applications that require experimentation using specific chemical end-groups. Chemical force microscopy (CFM) uses tips with different chemistries, produced through covalent attachment of thin monolayers of alkane-silanes or alkane-thiols [31–39].

Throughout their development, the above techniques have been used extensively to study the complex nanomechanical properties of natural bio-materials. For example, measurement of the modulus of algal adhesives [41,42], the energy dissipation mechanisms of spider silk [43–45], and single modular protein unfolding in diatom mucilage [46–50]. By studying the energy dissipation mechanisms of different bioadhesives, Smith *et al*. [51] proposed that the toughness present in most bioadhesives originates from the repetitive breaking of intermediate "sacrificial bonds" that prevent severe damage to the central protein backbone under stress [51–53]. The incorporation of sacrificial bonds in bioadhesives creates a resilient system capable of dissipating large amounts of energy.

Here, cyprids were encouraged to explore and deposit footprints onto $–NH_2$ terminated glass—a surface that exhibits a high degree of footprint protein retention. Footprints of *S. balanoides* (Fig. 1A and B) have been observed previously on $–NH_2$ functionalized glass surfaces [15] and their morphology is shown in Fig. 1. Figure 1A is a single footprint on a $–NH_2$ terminated surface. High-resolution imaging revealed that the adhesive is porous and fibrillar in nature on $–NH_2$ glass with isolated chains and bundles of protein aggregates present in the network structure of footprints (Fig. 1B) [15].

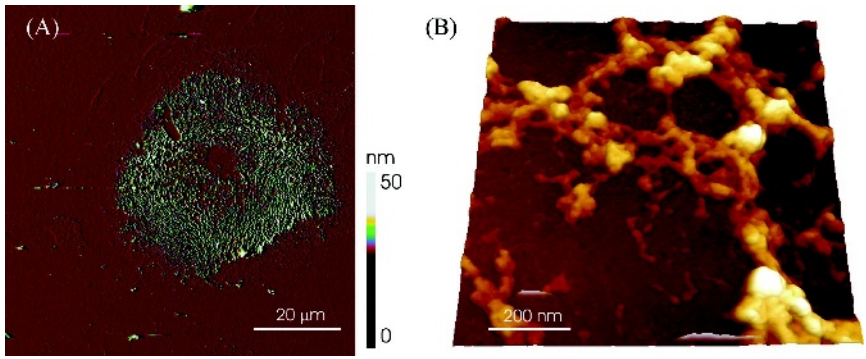

FIGURE 1 Atomic force microscopy (AFM) micrographs (deflection image) of cyprid larva footprints deposited on (A) $-NH_2$ chemically functionalized surfaces. (B) High resolution 3D AFM micrograph of protein adhesive in an aggregated fibrillar structure (scan size: $1 \times 1\,\mu m$ and z-range $= 50\,nm$).

Despite these recent advances, a quantitative understanding of the interactions between footprint proteins and surfaces is still lacking. Here, the interactions between footprint proteins, an $-NH_2$ substratum, and either hydrophobic or hydrophilic AFM tips are discussed.

EXPERIMENTAL

Animals

S. balanoides cyprids were collected by plankton tow from the wild population at Cullercoats, UK (55.1 N, 1.26 W) during April 2006 and were stored in 2 l glass containers, at 1 cyprid/mL, filled with artificial sea water (ASW; Tropic Marin^{TM}, Wartenberg, Germany) at 6°C prior to use. Feeding was not necessary as cyprids are lecithotrophic.

Chemicals

1-Octadecanethiol, [ODT, $CH_3(CH_2)_{17}SH$] and 3-aminopropyl triethoxysilane (APTES) were purchased from Sigma Aldrich, Zwijndrecht, The Netherlands. Chemicals were used as received.

Surface Preparation

Glass microscopy cover slips were sonicated in ethanol for 5 min and then immersed in piranha solution (a mixture of concentrated sulphuric acid and 33% hydrogen peroxide in a 3:1 ratio) for 15 mins. The surfaces were rinsed with nanopure water and dried under N_2. Amino (NH_2)-terminated surfaces were obtained by gas-phase evaporation of 3-aminopropyl triethoxysilane (APTES) in a desiccator under vacuum. Surfaces were incubated for several hours and then carefully rinsed with 99% ethanol and nanopure water. Contact angle measurements were carried out to characterize the functionalized surfaces immediately after completion of the silanization. The contact angle of NH_2-functionalized glass was 60°.

Preparation of Functionalized Tips

Triangular-shaped silicon nitride tips [Digital Instruments (DI), Santa Barbara, CA, USA] were coated with *ca*. 2 nm Ti and *ca*. 50 nm Au in high vacuum (SSENS b.v., Hengelo, NL). The cantilever functionalization was carried out as described earlier [54]. Briefly, the tips were sonicated in ethanol solution and rinsed with excess ethanol and distilled water. The tips were then incubated overnight in the thiolated

solution containing 1 mM of 1-octadecanethiol. The functionalized tips were rinsed thoroughly with ethanol and distilled water under a nitrogen stream. Surface wettability was 107° for the 1-octadecanethiol SAM.

Atomic Force Microscopy (AFM)

AFM measurements were carried out using a Dimension D3100 atomic force microscope equipped with a NanoScope IVa controller and a hybrid scanner (H-153) with x-, y-, z- feedbacks from Veeco [Veeco/Digital Instruments (DI), Santa Barbara, CA, USA]. Triangular-shaped silicon nitride cantilevers [Veeco/Digital Instruments (DI), Santa Barbara, CA, USA] were used throughout the study and cantilever spring constants were calibrated using the thermal noise method [55]. The cantilevers used for acquisition of the present results had a spring constant range from 0.062 to 0.100 N m. Cyprids were then deposited onto prepared surfaces by micro-pipette. Surfaces were mounted in glass Petri dishes prior to experimentation. Typically, cyprids would attach and begin to explore the surfaces when stimulated by small water currents. Explored areas of the glass were marked on the base of the cover slip and cyprids were then removed from the Petri dishes. Surfaces were flushed with a large amount of filtered ASW to minimize contamination and remained moist by ASW without exposure to air. Petri dishes were then transferred to the AFM and the search for footprints (FP) was focused on the marked regions. Custom programmed software for LABVIEW™ was used for data analysis throughout to transform the raw data to force-separation curves according to the method described by Janshoff *et al*. [26]. There were a total of 3860 pull-off events detected in 899 force extension curves from footprints on amine terminated glass (FP-NH_2) and 880 events were detected in 295 force-separation curves for statistical histogram presented in Fig. 2. Different chemically modified tips were used to measure the adhesion force of footprints deposited on NH_2-glass. All peaks were fitted with Lorentzian functions.

RESULTS AND DISCUSSION

Figure 3 shows typical force-extension curves obtained from AFM force measurements of footprints on -NH_2 functionalized glass surfaces using either commercial, untreated Si_3N_4-tips, or tips featuring an alkanethiol monolayer, terminated by $–CH_3$ functionalities (CH_3-tip hereafter). Force spectroscopy measurements were performed

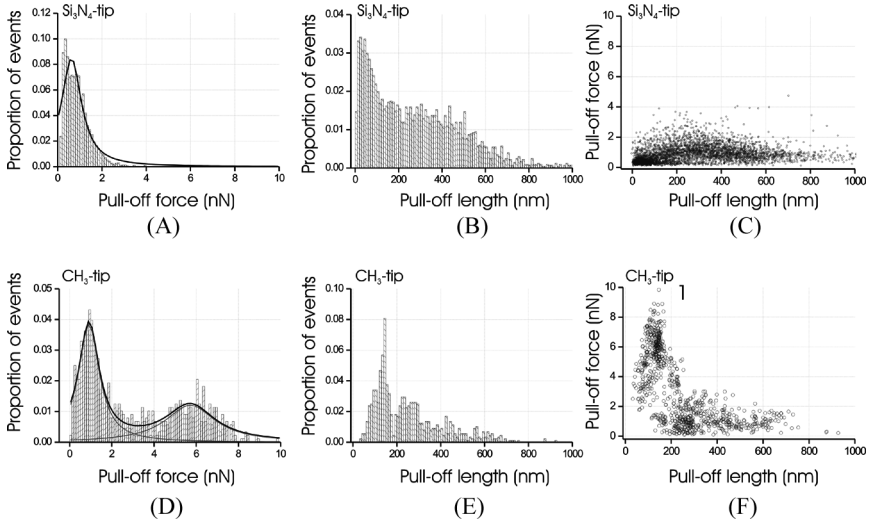

FIGURE 2 Histograms of pull-off force, pull-off length, and pull-off force *versus* pull-off length correlation plots from footprints found on NH_2-SAMs glass with (A–C) Si_3N_4-tip and (D–E) CH_3-tip. All peaks were fitted with Lorentzian functions.

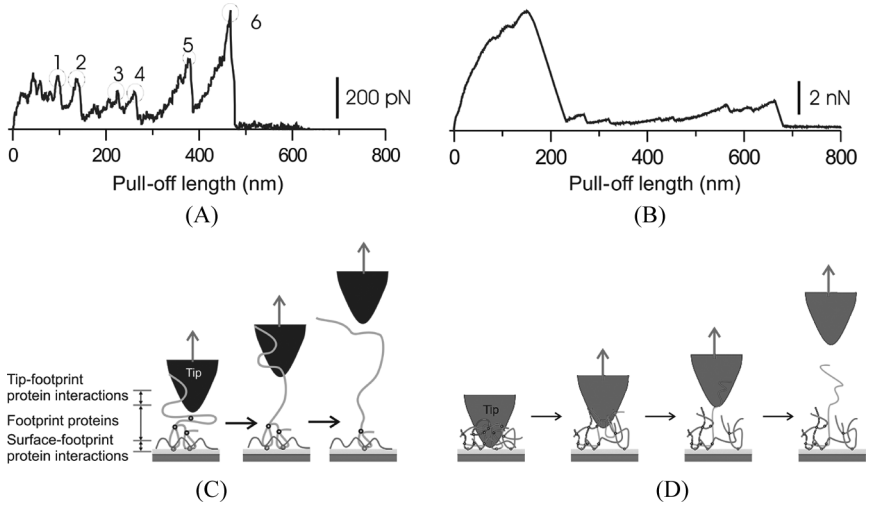

FIGURE 3 Representative force-separation curves between (A) FP-NH_2 and Si_3N_4-tip and (B) CH_3-tip. Only retraction cycle is shown in this figure. Note the difference in the scale of the pull-off force axis. Schematic of (C) Si_3N_4-tip and (D) CH_3-tip interacted with footprints found on NH_2-glass.

by allowing the AFM tip to contact and subsequently withdraw from the footprint surface. Force-extension curves (Figs. 3A and 3B) showed marked differences depending on the tip surface chemistry. In Fig. 3A, footprint proteins adhered to an untreated Si_3N_4 AFM tip and pull-off events were observed in the retraction cycle that rendered a saw-tooth appearance to the force-extension curve. Representative force curves consisted of sections of gradually increasing upward slopes as the protein chains experienced an increasing elongation towards their maximum extension. Eventually, a sacrificial bond, presumably involved in maintaining the tertiary structure of the protein, would yield and, as a consequence, the tension within the stretched chain dropped to a minimum, manifesting a "pull-off" event in the force-extension curve [56]. The chain length within the folded proteins unraveled as the sacrificial bonds were broken, which contributed to an increase in total extension of the protein. As the piezoelectric scanner was retracted further from the surface, the tip continued to stretch and unravel more sacrificial bonds [53]. As the stretching process continued, distinctive saw-tooth force curves were observed, which are known to be diagnostic of this type of unfolding behavior [57].

The process of sacrificial bond rupturing continued, presumably until the last sacrificial bond was broken. The saw-tooth characteristic was observed in both force extension curves obtained from Si_3N_4- and CH_3-tips. Figure 3B shows a typical force extension curve collected from a CH_3-tip acting upon FP-NH_2 (footprints deposited onto the $-NH_2$ substratum). For these hydrophobic tips, initially large pull-off forces were typically observed with a pull-off length of 100–200 nm, prior to the onset of the saw-tooth pattern, with pull-off peaks at much more moderate forces. The pull-off forces for CH_3-tips were considerably larger than for Si_3N_4-tips, with adhesion forces measuring up to several nanoNewtons (nN, 10^{-9} N) at the first part of the force-extension curve. Saw-tooth unfolding behavior then followed with pull-off forces of several hundreds of picoNewtons (pN, 10^{-12} N). The force and length recorded for each individual pull-off event (as shown in Fig. 3A, labels 1–6) were considered as individual pull-off force and pull-off length events in the subsequent analyses.

In our study, the footprint proteins were freshly secreted by cyprids with neither additional treatment nor purification. Thus, it is likely that at least some of the observed stretching events were the result of bundles of protein aggregates binding to the AFM tip, connected to each other *via* sacrificial bonds. In the present context, therefore, sacrificial bond refers to all of the possible supramolecular intra- and intermolecular (non-covalent) bonds within the footprint material that maintain its conformation in native conditions [51,52].

The pull-off force measurements from control experiments on NH_2-glass (without footprints) were obtained using a CH_3-tip, as well as a Si_3N_4-tip. All the force-distance curves showed a single adhesion pull-off peak in the control experiments. The respective histograms of the pull-off forces indicated adhesion forces of 1.1 ± 0.2 and 2.2 ± 0.4 nN, for Si_3N_4 and CH_3-tips, respectively. This trend is in line with measurements taken using functionalized tips in water (see review by Noy *et al.* [36]). As these single-peaked adhesion-force curves were observed at very low pull-off lengths (in comparison with the footprint proteins), it is considered that any effect of the substratum on the present adhesion measurements was negligible. Further, this technique confirmed that no FP proteins remained on the used tips after experiments.

Figures 3C and D show the mechanism that is believed to operate during the stretching of FP proteins with the Si_3N_4 and CH_3-tips, respectively. For a hydrophilic tip, the nonspecific pull-off forces are moderate and the pull-off cycle is dominated by the rupturing of sacrificial bonds. This indicates that relatively few protein strands adhere to the tip on any one pulling cycle. In contrast, it appears that adhesion of FP material to the CH_3-tip is dominated by strong hydrophobic interactions, with many proteins adhering to the tip on initial contact. When the hydrophobic tip approached the FP material, water was excluded from the interface and protein strands adhered nonspecifically to the tip. This observation assumes that the conformational change and denaturing of the protein would facilitate hydrophobic interaction by enhancing contact forces between CH_3-functionalized tips and hydrophobic groups in the footprint molecule [36,58]. Following the sacrificial rupture model, fibrils remaining attached to the tip on the retraction cycle unfolded until, eventually, the weakest link was ruptured and contact between FP proteins and tip was lost (*e.g.,* label 6 in Fig. 3A).

As shown in Figs. 3(A–B), the FP proteins were anchored securely to the tip prior to detachment. Hence, individual sacrificial bond strengths and the interactions between FP proteins and the substratum could be examined. As the pulling process continued, the sacrificial bonds broke and the chain was stretched further until it finally detached from the tip (Figs. 3C–D).

Force curves summarizing the nanomechanical properties of footprint proteins are included in Fig. 2. Figures 2A–C are histograms of the pull-off force, the pull-off length, and pull-off force *versus* pull-off length for FP proteins measured using a Si_3N_4-tip from FP-NH_2. The pull-off forces required to stretch proteins from FP-NH_2 substrates (Fig. 2A) were broadly distributed around one peak at 0.7 nN. This was

identified using a single Lorentzian fit. The corresponding pull-off lengths presented in Fig. 2B showed a narrowly distributed population with an average length of 40 nm and a very broad population peaked at ~280 nm. The force histograms obtained with CH_3-tips (Fig. 2D), by comparison, exhibited a distribution with two Lorentzian peaks with maxima at 0.9 and 6 nN. The high pull-off force peak, in particular, exhibited a very broad distribution, ranging from 2–8 nN. The histogram of the pull-off length from CH_3-tips is shown in Fig. 2E. Again, a sharp maximum at short pull-off lengths (~40 nm) and a broad distribution centered on 400 nm can be observed.

The cross-correlation plots in Figs. 2C and F provided a better understanding of the behavior of the footprint material under strain. In a single force cycle, several pull-off events were often observed at different rupture lengths before the final detachment of the protein from the tip. In the case of Si_3N_4-tips (Fig. 2C), rupture forces were confined to the range 0–2 nN, while corresponding pull-off lengths varied between 0–800 nm. This result suggested that for Si_3N_4-tips, at least, the force required to extend footprint proteins, or bundles thereof, was not directly dependent on the potential maximum extension length of those proteins. The force required for extension was likely the force required to rupture inter-molecular sacrificial bonds, which would be consistent anywhere in the strain-cycle, rather than a result of elastic deformation of the test material. Pull-off events were most densely clustered at the low end of the 0–800 nm x-axis (Fig. 2C). Both of these observations are supportive of our hypothesis that few proteins attached to the Si_3N_4-tips and that their adhesion was also relatively weak.

Figure 2F shows the correlation with respect to $–CH_3$ functionalized tips. In this case, two populations were clearly visible—namely, a horizontal band similar to that observed for the Si_3N_4-tip (Fig. 3C) and a separate vertical peak of high force at short pull-off lengths (up to 10 nN). This second population of high pull-off forces relates to the high adhesion recorded in some force-cycles with the CH_3-tip (Fig. 3B). The low pull-off forces observed using the CH_3-tip (0.9 nN) were similar to the forces observed using the Si_3N_4-tip (0.7 nN). Hence, we ascribe the high recorded forces, present only when the CH_3-tip was used, to nonspecific hydrophobic interactions between the CH_3-tip and the FP material and the lower forces, present when both tips were used, to the breaking of sacrificial bonds in the FP material.

The CH_3-tip correlation plot (Fig. 2F) showed that high pull-off force events were mostly concentrated at low pull-off lengths—*i.e.,* on initial contact/removal of the tip with/from the FP material. The

average pull-off force observed for the hydrophobic CH_3-tip (~6 nN) was approximately one order of magnitude higher than the average pull-off force for the hydrophilic Si_3N_4-tip in this situation. Although the CH_3 monolayer was deposited onto a gold substrate on the tip, and there is potential for specific interactions between gold and putative disulfide groups in the FP material, these interactions are unlikely to be responsible for the increased force as the CH_3 monolayer was densely packed and no gold would have been exposed to the footprint [59].

Our explanation for the improved adhesion to CH_3-tips, therefore, is in the form of simple hydrophobic attraction. If, as is likely, the free energies of the footprint and the CH_3-tip were far below that of seawater, the seawater at the tip-FP interface would have been excluded when the two were brought into contact. The surface tension of the seawater would prevent it from preferentially wetting either of the two materials and the tip and the footprint would, therefore, be forced together under pressure from the surrounding medium. Van der Waals-type forces presumably assist in maintaining the adhesion [31,36,60–63]. Such a scenario could not occur with the Si_3N_4-tip as the difference in free energy between this material and seawater is much less [65]. $-CH_3$-terminated surfaces in water have previously been reported to show 10–20 times higher pull-off forces compared with $-CH_2OH$-terminated surfaces [36,61].

Presumably these observations could have serious implications for the development of fouling-release coatings where, on the macro-scale, fouling can be removed more easily from low surface energy materials [65–68]. However, micro-scale bioadhesion, in this case at least, appears to be enhanced on low energy materials. The phenomenon described here could go some way to explaining the paradoxically successful growth of microalgae and bacteria on low-energy anti-fouling materials, but could also suggest some disparity between surfaces to which cyprids and adult barnacles attach most tenaciously.

A hydrophobic adhesive material would have numerous benefits over a hydrophilic one for use in an aqueous medium. Not least is that it would be less likely to be dissolved by the surrounding seawater and that it could serve as an effective water-excluder, allowing interaction between the cuticular villi on the base of the cyprid attachment disc with the surface as proposed by Phang *et al.* [15]. It is possible, therefore, that cyprids do in fact adhere to surfaces in a similar way to flies and some other insects [69], despite being surrounded by water, and this provides a direction for future research into biomimetic underwater adhesives [7,70]. This study has demonstrated that the footprint material of cyprids of *S. balanoides* has greater affinity to hydrophobic

surfaces, contrary to what is understood of the adhesives of adults of this species—although there remains the possibility of inter-species variability in this regard. It is unlikely that evolution would craft a sessile organism whose two life stages required different substratum characteristics for maximal adhesion, so this again supports the hypothesis that the FP material is not an adhesive *per se*, but that it contributes to a more complex adhesive system. It is entirely possible that the temporary adhesive system of cyprids, taken in its entirety, may manifest stronger attachment to high-energy surfaces, as might be expected, although this remains to be investigated thoroughly.

CONCLUSIONS

The mechanical behavior of barnacle cyprid (*Semibalanus balanoides*) footprint proteins was probed using AFM tips with specific chemistries. Footprints deposited onto NH_2-terminated glass were imaged and tensile-tested *in situ* by AFM. Data from footprints probed with a $–CH_3$ tip were clearly bimodal in terms of pull-off force (Fig. 3D) and it is concluded that the cluster of data points at higher force represented hydrophobic adhesion of proteins to the tip at the footprint surface. The points at lower force were likely to be related to the unfolding of the tertiary structure of the proteins and breaking of sacrificial bonds. Only the latter group was present when a Si_3N_4-tip was used.

We explain this as follows. When the tip (with either chemistry) was brought into contact with the FP surface, FP proteins adhered to it. On retraction, more proteins adhered to the $–CH_3$ tip than to the Si_3N_4-tip, manifesting a peak in pull-off force close to the FP surface when the $–CH_3$ tip was used. This force was the result of a combination of numerous attached proteins. As the retraction cycle commenced, proteins detached from the $–CH_3$ tip, resulting in single or a few proteins unfolding and finally detaching from the tip at maximum extension. For Si_3N_4, few proteins adhered to the tip while it was in contact with the FP surface and, therefore, no "breakaway" peak was observed, only the unfolding and detachment of single/few protein chains as for $–CH_3$. Correlation plots (Fig. 2C and F) confirmed that the high force measurements for the $–CH_3$ tip all occurred at low pull-off length, suggesting that multiple proteins were sticking to the tip simultaneously when it was brought into contact with the footprint surface. This did not occur with the Si_3N_4-tip. Footprint proteins, in an aqueous medium, therefore, had a greater affinity to the $–CH_3$ tip than to the Si_3N_4-tip and this can only be easily explained if the footprint protein is predominantly hydrophobic.

ACKNOWLEDGMENTS

Present research is supported by a Dutch Polymer Institute grant #DPI–510 (to G.J.V.). Nick Aldred was supported by U.S. Office of Naval Research grants (N00014-05-1-0767 and N00014-08-1-1240) to A.S.C.

REFERENCES

[1] Christie, A. O. and Dalley, R., Barnacle fouling and its prevention, in *Crustacean Issues 5: Barnacle Biology*, A. J. Southward (Ed.) (Balkema, Rotterdam, 1987), pp. 419–433.
[2] Schultz, M. P., *Biofouling* **23**, 331–341 (2007).
[3] Yebra, D. M., Kiil, S., and Dam-Johansen, K., *Prog. Org. Coat.* **50**, 75–104 (2004).
[4] Townsin, R. L., *Biofouling* **19**, 9–15 (2003).
[5] Kamino, K., *Mar. Biotechnol.* **10**, 111–121 (2008).
[6] Crisp, D. J., Walker, G., Young, G. A., and Yule, A. B., *J. Colloid Interface Sci.* **104**, 40–50 (1985).
[7] Aldred, N. and Clare, A. S., *Biofouling* **24**, 351–363 (2008).
[8] Walker, G. and Yule, A. B., *J. Mar. Biol. Ass. U.K.* **64**, 679–686 (1984).
[9] Clare, A. S. and Nott, J. A., *J. Mar. Biol. Ass. U.K.* **74**, 967–970 (1994).
[10] Nott, J. A. and Foster, B. A., *Philos. Trans. R. Soc. Lond., Ser. B* **256**, 115–134 (1969).
[11] Walker, G., *J. Adhes.* **12**, 51–58 (1981).
[12] Yule, A. B. and Walker, G., in *Crustacean Issues 5: Barnacle Biology*, A. J. Southward (Ed.) (A. A. Balkema, Rotterdam, 1987), pp. 389–402.
[13] Bandyopadhyay, P. R., Hrubes, J. D., and Leinhos, H. A., *Bioinspir. Biomim.* **3**, 016003 (2008).
[14] Aldred, N., Phang, I. Y., Conlan, S. L., Clare, A. S., and Vancso, G. J., *Biofouling* **24**, 97–107 (2008).
[15] Phang, I. Y., Aldred, N., Clare, A. S., Callow, J. A., and Vancso, G. J., *J. R. Soc. Interface* **5**, 397–401 (2008).
[16] Phang, I. Y., Chaw, K. K., Choo, S. S. H., Kang, R. K. C., Lee, S. S. C., Birch, W. R., Teo, S. L. M., and Vancso, G. J., *Biofouling* **25**, 139–147 (2009).
[17] Gerber, C. and Lang, H. P., *Nat. Nanotechnol.* **1**, 3–5 (2006).
[18] Engel, A. and Muller, D. J., *Nat. Struct. Biol.* **7**, 715–718 (2000).
[19] Radmacher, M., Tillmann, R. W., Fritz, M., and Gaub, H. E., *Science* **257**, 1900–1905 (1992).
[20] Butt, H. J., Cappella, B., and Kappl, M., *Surf. Sci. Rep.* **59**, 1–152 (2005).
[21] Cappella, B. and Dietler, G., *Surf. Sci. Rep.* **34**, 1–104 (1999).
[22] Ginger, D. S., Zhang, H., and Mirkin, C. A., *Angew. Chem. Int. Ed.* **43**, 30–45 (2004).
[23] Jaschke, M. and Butt, H. J., *Langmuir* **11**, 1061–1064 (1995).
[24] Carrion-Vazquez, M., Oberhauser, A. F., Fisher, T. E., Marszalek, P. E., Li, H. B., and Fernandez, J. M., *Prog. Biophys. Mol. Biol.* **74**, 63–91 (2000).
[25] Hinterdorfer, P., Baumgartner, W., Gruber, H. J., Schilcher, K., and Schindler, H., *Proc. Natl. Acad. Sci. U.S.A.* **93**, 3477–3481 (1996).
[26] Janshoff, A., Neitzert, M., Oberdorfer, Y., and Fuchs, H., *Angew. Chem. Int. Ed.* **39**, 3213–3237 (2000).
[27] Lee, G. U., Chrisey, L. A., and Colton, R. J., *Science* **266**, 771–773 (1994).

[28] Mitsui, K., Hara, M., and Ikai, A., *FEBS Lett.* **385**, 29–33 (1996).
[29] Moy, V. T., Florin, E. L., and Gaub, H. E., *Science* **266**, 257–259 (1994).
[30] Schonherr, H., Beulen, M. W. J., Bugler, J., Huskens, J., van Veggel, F., Reinhoudt, D. N., and Vancso, G. J., *J. Am. Chem. Soc.* **122**, 4963–4967 (2000).
[31] Frisbie, C. D., Rozsnyai, L. F., Noy, A., Wrighton, M. S., and Lieber, C. M., *Science* **265**, 2071–2074 (1994).
[32] Noy, A., *Surf. Interface Anal.* **38**, 1429–1441 (2006).
[33] Hudson, J. E. and Abruna, H. D., *J. Am. Chem. Soc.* **118**, 6303–6304 (1996).
[34] McKendry, R., Theoclitou, M. E., Rayment, T., and Abell, C., *Nature* **391**, 566–568 (1998).
[35] Vezenov, D. V., Noy, A., Rozsnyai, L. F., and Lieber, C. M., *J. Am. Chem. Soc.* **119**, 2006–2015 (1997).
[36] Noy, A., Vezenov, D. V., and Lieber, C. M., *Annu. Rev. Mater. Sci.* **27**, 381–421 (1997).
[37] Sheng, X. X., Jung, T. S., Wesson, J. A., and Ward, M. D., *Proc. Natl. Acad. Sci. U.S.A.* **102**, 267–272 (2005).
[38] Hillborg, H., Tomczak, N., Olah, A., Schonherr, H., and Vancso, G. J., *Langmuir* **20**, 785–794 (2004).
[39] Vancso, G. J., Hillborg, H., and Schonherr, H., Chemical composition of polymer surfaces imaged by atomic force microscopy and complementary approaches, in *Polymer Analysis, Polymer Theory*, (Springer, Berlin, 2005), Vol. 182, pp. 55–129.
[40] Giannotti, G. I. and Vancso, G. J., *Chem. Phys. Chem*. **8**, 2290–2307 (2007).
[41] Mostaert, A. S. and Jarvis, S. P., *Nanotechnology* **18**, 044010 (2007).
[42] Walker, G. C., Sun, Y. J., Guo, S. L., Finlay, J. A., Callow, M. E., and Callow, J. A., *J. Adhes.* **81**, 1101–1118 (2005).
[43] Becker, N., Oroudjev, E., Mutz, S., Cleveland, J. P., Hansma, P. K., Hayashi, C. Y., Makarov, D. E., and Hansma, H. G., *Nat. Mater.* **2**, 278–283 (2003).
[44] Oroudjev, E., Soares, J., Arcdiacono, S., Thompson, J. B., Fossey, S. A., and Hansma, H. G., *Proc. Natl. Acad. Sci. U.S.A.* **99**, 6460–6465 (2002).
[45] Shulha, H., Po Foo, C. W., Kaplan, D. L., and Tsukruk, V. V., *Polymer* **47**, 5821 (2006).
[46] Crawford, S. A., Higgins, M. J., Mulvaney, P., and Wetherbee, R., *J. Phycol.* **37**, 543–554 (2001).
[47] Dugdale, T. M., Dagastine, R., Chiovitti, A., Mulvaney, P., and Wetherbee, R., *Biophys. J.* **89**, 4252–4260 (2005).
[48] Dugdale, T. M., Dagastine, R., Chiovitti, A., and Wetherbee, R., *Biophys. J.* **90**, 2987–2993 (2006).
[49] Dugdale, T. M., Willis, A., and Wetherbee, R., *Biophys. J.* **90**, L58-L60 (2006).
[50] Higgins, M. J., Molino, P., Mulvaney, P., and Wetherbee, R., *J. Phycol.* **39**, 1181–1193 (2003).
[51] Smith, B. L., Schaffer, T. E., Viani, M., Thompson, J. B., Frederick, N. A., Kindt, J., Belcher, A., Stucky, G. D., Morse, D. E., and Hansma, P. K., *Nature* **399**, 761–763 (1999).
[52] Groshong, K., *New Scientist* **194**, 43–45 (2007).
[53] Fantner, G. E., Oroudjev, E., Schitter, G., Golde, L. S., Thurner, P., Finch, M. M., Turner, P., Gutsmann, T., Morse, D. E., Hansma, H., and Hansma, P. K., *Biophys. J.* **90**, 1411–1418 (2006).
[54] Schonherr, H., Hruska, Z., and Vancso, G. J., *Macromolecules* **31**, 3679–3685 (1998).
[55] Hutter, J. L. and Bechhoefer, J., *Review of Scientific Instruments* **64**, 1868–1873 (1993).

[56] Phang, I. Y., Aldred, N., Clare, A. S., Callow, J. A., and Vancso, G. J., *Biofouling* **22**, 245–250 (2006).
[57] Li, H. B., Linke, W. A., Oberhauser, A. F., Carrion-Vazquez, M., Kerkviliet, J. G., Lu, H., Marszalek, P. E., and Fernandez, J. M., *Nature* **418**, 998–1002 (2002).
[58] Zardeneta, G., Mukai, H., Marker, V., and Milam, S. B., *J. Oral Maxillofac. Surg.* **54**, 873–878 (1996).
[59] Carl, P., Kwok, C. H., Manderson, G., Speicher, D. W., and Discher, D. E., *Proc. Natl. Acad. Sci. U.S.A.* **98**, 1565–1570 (2001).
[60] Singh, S., Houston, J., van Swol, F., and Brinker, C. J., *Nature* **442**, 526–526 (2006).
[61] Sinniah, S. K., Steel, A. B., Miller, C. J., and Reutt-Robey, J. E., *J. Am. Chem. Soc.* **118**, 8925–8931 (1996).
[62] Skulason, H. and Frisbie, C. D., *Langmuir* **16**, 6294–6297 (2000).
[63] Meyer, E. E., Rosenberg, K. J., and Israelachvili, J., *Proc. Natl. Acad. Sci. U.S.A.* **103**, 15739–15746 (2006).
[64] Israelachvili, J. N., *Intermolecular and Surface Forces*, (Academic Press, London, 1991), p. 480.
[65] Lindner, E., *Biofouling* **6**, 193–205 (1992).
[66] Callow, M. E. and Fletcher, R. L., *Int. Biodeterior. Biodegrad.* **34**, 333–348 (1994).
[67] Swain, G. W. and Schultz, M. P., *Biofouling* **10**, 187–197 (1996).
[68] Brady, R. F. and Singer, I. L., *Biofouling* **15**, 73–81 (2000).
[69] Niederegger, S., Gorb, S., and Jiao, Y. K., *J. Comp. Physiol. A.* **187**, 961–970 (2002).
[70] Clare, A. S. and Aldred, N., in *Advances in Marine Antifouling Coatings and Technologies*, C. Hellio and D. M. Yebra (Eds.) (Woodhead Publishing Ltd., Cambridge, 2009).